11th International Symposium on Turbulence and Shear Flow Phenomena (TSFP11)
Southampton, UK, July 30 to August 2, 2019

BAYESIAN OPTIMISATION OF INTERMITTENT WALL BLOWING IN A TURBULENT BOUNDARY LAYER FOR NET POWER SAVING

Omar A. Mahfoze
Department of Aeronautics
Imperial College London
London SW7 2AZ, UK
omar.mahfoze15@imperial.ac.uk

Andrew Wynn
Department of Aeronautics
Imperial College London
London SW7 2AZ, UK
a.wynn@imperial.ac.uk

Richard D. Whalley
School of Engineering
Newcastle University,
Newcastle NE1 7RU, UK
richard.whalley@newcastle.ac.uk

Sylvain Laizet
Department of Aeronautics
Imperial College London
London SW7 2AZ, UK
s.laizet@imperial.ac.uk

ABSTRACT

A Bayesian optimisation framework is used to optimise low-amplitude wall-normal blowing control of a turbulent boundary-layer (TBL) flow in order to achieve skin-friction drag reduction and net-power saving. The study is carried out using Direct Numerical Simulations (DNS) and Implicit Large Eddy Simulations (ILES). Control performance is assessed by using the power consumption from two different sets of experimental data from two different types of blowing device. The simulations demonstrate that wall-normal blowing control can generate a local skin-friction drag reduction of up to 75%, which persists far downstream of the control. This slow spatial recovery of the skin-friction coefficient back to its canonical counterpart can generate net-power savings up to 5% in the present study. When combined with DNS or ILES, Bayesian optimisation, with its fast convergence (within a dozen iterations with three parameters to optimise) is an ideal tool to find the optimal set of parameters to maximise net-power saving. The evolution of the skin-friction coefficient is decomposed using the Fukagata-Iwamoto-Kasagi (FIK) identity, which shows that the generation of the net-power savings is due to changes in contributions to both the convection and streamwise development terms of the turbulent boundary-layer flow.

INTRODUCTION

Skin-friction drag reduction is a topic of great interest due to its importance in many engineering applications. As an example, just a 3% reduction in the skin-friction of a long-range commercial aircraft would save £1.2m in jet fuel per aircraft per year and prevent the annual release of 3,000 tonnes of carbon dioxide. Despite many decades of extensive research, a practical and affordable method for skin-friction drag reduction is yet to be found and implemented in real-world applications. Various strategies, which include polymer additives, riblets, vibrators, microelectromechanical systems, gas microbubbles, hydrophobic coating and large eddy breakup devices have been developed in the last decades to reduce skin-friction drag. Adding polymer additives to a liquid flow, for instance, can reduce skin-friction drag by more than 70%, yielding a phenomenon known as Maximum-Drag-Reduction (Virk (1975)). For air flows, however, the energy expenditure of typical active drag reduction strategies can be very high, often leading to net-power loss even if substantial skin-friction drag reduction is obtained.

In the present work we focus on the spatial development of a zero pressure gradient turbulent boundary layer and the resulting wall friction after control has been applied locally using vertical wall-blowing as a drag-reducing strategy. It is well know that low-amplitude wall-normal blowing (less than 1% of the free stream velocity) can substantially reduce skin-friction drag. Recent simulations by Kametani & Fukagata (2011) and Stroh *et al.* (2016) have shown that it is possible to achieve up to 60% local skin-friction reduction with uniform blowing at moderate Reynolds numbers, which persists to tens of boundary-layer thicknesses downstream of the control. A series of Large-Eddy Simulations (LES) of turbulent boundary-layer flows with wall-normal blowing control were performed by Kametani *et al.* (2016) with a focus on the effect of intermittent blowing along the direction of the flow. By considering only part of the input power required to generate the wall-blowing, namely the pressure difference across the blowing wall, a very optimistic idealised net-power saving of around 18% was predicted.

Employing a reliable optimisation method to determine the optimal parameters of a vertical wall-blowing control technique could potentially lead to substantial net-power saving. Bayesian Optimisation (BO) is a derivative-free algorithm that works efficiently with expensive non-convex objective functions (Gelbart *et al.* (2014)). BO plays a prominent role in efficiently optimising the parameters of machine learning algorithms, such as Neural Networks, with superior performance when compared to more standard approaches (Snoek *et al.* (2012); Brochu *et al.* (2010)). BO is yet to be used for fluid flow problems and very few

studies combining DNS/LES and BO have been published to date.

BAYESIAN OPTIMISATION

In the present study, a Bayesian Optimisation (BO) algorithm is used to achieve drag reduction and net-power saving. Generically, BO algorithms seek to minimise a chosen objective function over a given set of parameter values based on previous observations. BO algorithms have two stages. First, given knowledge of the objective at a known set of parameters, a probability density function for the objective function (in our case, the objective function is the net-power saving, also known as *posterior*) is computed. This encapsulates a *best guess* of the objective and quantifies the uncertainty of the approximation. Second, an *acquisition function* is minimised to determine the next set parameter values to be sampled. This typically involves a trade-off between minimising the expected objective and reducing the uncertainty of its approximation.

For a simple illustrative example of the BO algorithm, consider a 1D problem that has a noise-free objective function, $f(x) = -\sin(x)/x$, for $-2 \leq x \leq 1$. Figure 1 shows the development of the *posterior* distribution over four iterations of the BO algorithm. Near the training points (black markers), the posterior mean (red curve) and the true function (black curve) match and the posterior uncertainty vanishes; conversely, the uncertainty of the predictive model increases with distance from the observation points. The first new input parameter x_2 (figure 1 b) corresponds to the lowest value of the posterior mean. Subsequently, since x_2 is close to the lowest value of the new posterior mean (almost unchanged from the previous figure), the BO algorithms selects a testing point x_3 (figure 1 c) in a region of high uncertainty. As it can be seen for this small example, the true minimum of the objective function is found very quickly.

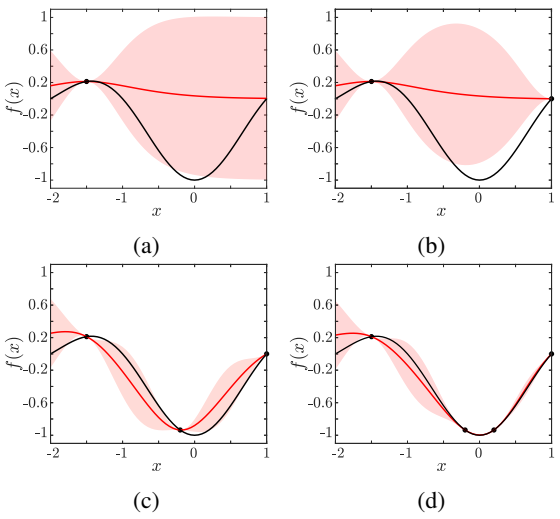

Figure 1: An example of using Bayesian Optimisation to find a local minimum on a 1*D* toy problem. The black curve is the true objective function, black solid circles are the observed points, the red curve is the posterior mean and the red shaded area is the posterior uncertainty.

NUMERICAL METHODS

In order to generate the data for the BO studies, simulations of a turbulent boundary layer need to be performed efficiently. The incompressible Navier-Stokes equations are solved on Cartesian mesh using the high-order flow solver `Incompact3d`, which has been adapted to parallel supercomputers using a powerful two-dimensional (2D) domain decomposition strategy (Laizet & Li (2011)). The equations are spatially discretised using sixth-order finite-difference schemes, and a second-order semi-implicit scheme for the time advancement. The Poisson equation, which is required to satisfy the incompressibility condition, is solved in spectral space to avoid expensive iterative solvers. More details about `Incompact3d` can be found in (Laizet & Lamballais, 2009). Note that it has been used recently for DNS of turbulent boundary-layer flows for a detailed wall-shear stress study (Diaz-Daniel *et al.* (2017)). The present simulations are performed on a domain size $L_x \times L_y \times L_z = (750 \times 40 \times 15)\delta_0$, where L_x, L_y and L_z are the streamwise, vertical and spanwise directions, respectively, as seen in figure 2. δ_0 is the thickness of the boundary layer at the inlet. A Blasius profile with $Re_\theta = 170$ (based on the momentum thickness θ and the free stream velocity U_∞) is imposed at the inlet, followed by a tripping zone in order to trigger turbulence transition. Periodic boundary conditions are applied in the spanwise direction, Neumann conditions are applied at the top boundary and 1D convection equation is solved for the outlet boundary condition. No-slip boundary condition is applied at the wall except in the control region which extends between $Re_\theta = 470 : 700$ where the normal velocity can be non-zero. For the canonical case, $Re_\theta \approx 2100$ at the end of the domain.

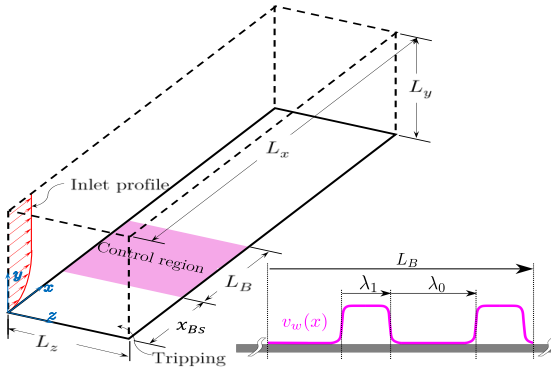

Figure 2: Schematic of the computational domain (left), and the wall normal velocity in the control region (right)

Small-amplitude wall-normal blowing is applied to the turbulent boundary-layer flow in search of a wall-normal blowing control strategy which would yield a skin-friction drag reduction with a net-power saving. The BO algorithm is used to search over three control parameters simultaneously. The parameters chosen for this study are the wall-normal blowing coefficient $C_B = v_w/U_\infty$ (v_w is the vertical velocity at the wall), the number of streamwise blowing areas within the control area of streamwise extent L_B, N_B and the blowing coverage coefficient, $\alpha = \lambda_1 N_B/L_B$. As seen in figure 2, steady wall-normal blowing is applied uniformly in the spanwise direction, across the full extent of the control area, with λ_1 and λ_0 denoting the streamwise extent of blowing and non-blowing sections, respectively. The control region is located at a distance $x_{Bs} = 68\delta_0$ from the in-

let with a streamwise extent $L_B = 77\delta_0$, corresponding to $470 \leq Re_\theta \leq 700$ in the canonical flow.

In the first part of this study, the BO is using Direct Numerical Simulation (DNS). The computational domain is discretised using $n_x \times n_y \times n_z = 3073 \times 321 \times 128$ mesh nodes. The mesh size in wall viscous units for $Re_\theta = 365$ is $\Delta x^+ = 16.6, \Delta y^+ = 0.53 : 135.5$ and $\Delta z^+ = 8$ in the streamwise, normal and spanwise directions, respectively. The second part of the study is based on Implicit Large Eddy Simulations (ILES). The compact finite-difference schemes used in `Incompact3d` can be modified at no extra cost in order to add some artificial dissipation at the small scales using the numerical error of the schemes (Dairay *et al.* (2017)). It is possible to control the amount of artificial dissipation near the cut-off wave number and for the present study, it was found that the artificial viscosity is nine times the value of the physical viscosity (only at the small scales) in order to get the same quality of results between the DNS and the ILES. The computational domain for the ILES is discretised using $n_x \times n_y \times n_z = 1537 \times 257 \times 64$ mesh nodes. The mesh size in wall viscous units for $Re_\theta = 365$ is $\Delta x^+ = 33, \Delta y^+ = 0.57 : 500$ and $\Delta z^+ = 16$ in the streamwise, normal and spanwise directions, respectively. Additionally, the ILES time step is twice the DNS time step so the cost of a ILES is 16 times less than the cost of a DNS.

Net-power Saving

The net-power saving S generated by each wall-normal blowing control strategy is assessed by taking into account the input power required to generate the wall-normal blowing plus any power saving due to a reduction in skin-friction drag. Due to the long-lasting downstream effects of the low-amplitude wall-normal blowing control, a global skin-friction drag coefficient C_f is evaluated over a streamwise distance $L = 615\delta_0$ with

$$C_f = \frac{1}{L}\int_{35\delta_0}^{650\delta_0} c_f(x)dx. \quad (1)$$

The reduction in C_f is referred to as the global drag reduction (GDR). The net-power saving S is defined as

$$S = \frac{C_w - C_{w0}}{C_{w0}}, \quad (2)$$

where C_{w0} is the power coefficient of the canonical case. The gross power input coefficient for controlled case $C_w = C_{w\tau} + C_{wb}$ is equal to the sum of the mean viscous power coefficient $C_{w\tau}$ to overcome the shear stress, and the blowing power coefficient C_{wb}. In our simulations the blowing is imposed via a boundary condition at the wall for the vertical velocity. As a result, C_{wb} can only be estimated using experimental data, in our study from two different blowing systems. The first system Sys_1 was developed by Kornilov & Boiko (2012). It is based on a pressurised chamber on one side of a micro-drilled plate to blow air with low intensity. A relationship between the pressure drop through the plate and C_B was provided, however, the authors did not indicate the power required to compress the air in their system. For Sys_1, only the pressure drop is taken into account so the blowing power estimation is not really accurate. C_{wb} is expressed as

$$C_{wb} = (C_p C_B + C_B^3)\alpha_t, \quad (3)$$

where α_t is the ratio of the blowing region to the total area over which the global drag is calculated. C_p is the pressure coefficient of the pressure difference across the permeable wall. The pressure coefficient C_p was measured at a free-stream velocity of $U_\infty = 21m/s$ and is proportional to the wall-normal blowing amplitude, with $C_p = 124C_B$.

The second system Sys_2 is currently being developed at the University of Newcastle (UK) and is based on miniature electromagnetic speakers to blow low-intensity air across a micro perforated plate. The instantaneous total power input for the speakers as a function of the blowing velocity is used to compute the potential net-power saving. Based on experimental data, the averaged speaker power P_B per unit area A as function of the wall normal velocity v_w is $P_B/A = 3169v_w^3 - 970.3v_w^2 + 256.2v_w$ and

$$C_{wB} = \frac{P_B}{\frac{1}{2}U_\infty^3 A_t}. \quad (4)$$

A_t is the total area over which the global drag reduction is estimated. This relation is used to estimate the net-power saving for Sys_2 with an accurate calculation of the power associated with the speaker-based wall blowing device.

RESULTS AND DISCUSSION

The main goal of this study is to evaluate the ability of a Bayesian Optimisation (BO) framework fed by DNS data to find an optimal set of parameters to achieve substantial drag reduction and/or net-power saving for a turbulent boundary layer using a wall blowing device. The drag reduction mechanisms from the most promising sets of parameters will be investigated using the well-known Fukagata-Iwamoto-Kasagi (FIK) identity. Furthermore, we will also see if it is possible to use ILES data instead of DNS data to feed the BO framework in order to reduce the cost of the optimisation. Finally, we will investigate the potential of a time modulation for the wall blowing with the aim to reduce the cost of the blowing and potentially generate higher levels of net-power saving.

BO study based on DNS

Two Bayesian optimisation studies are conducted based on the experimental data Sys_1 (BO1) and Sys_2 (BO2). The associated net-power saving is referred to as S_1 and S_2, respectively. Table 1 and Table 2 summarises the blowing parameters, the maximum local drag reduction , the mean drag reduction over L and net-power saving (a negative sign is associated to an energy loss). For both studies, the first three cases 1,2 and 3 have parameters that are selected arbitrarily while case 0 correspond to a canonical TBL with no control.

18 DNS were performed for BO1 with the aim to optimise the net-power saving (not the global drag reduction). It can be seen that after 14 DNS the data are converged with virtually no change in the net-power saving for the last 4 DNS. As seen in table 1, BO1 predicts that uniform blowing with low wall velocity ($v_w \approx 0.3\%$ of U_∞) would lead to a net-power saving of 5% with an averaged drag reduction over L of $\approx 8\%$ and a local maximum drag reduction of $\approx 36\%$ (Case 13 in blue). As it can be seen for Case 5 (in red), more than 75% of local drag reduction can be achieved however with a substantial energy loss of nearly 10%. It is important to mention that for Sys_1, the power calculation for

Table 1: Wall-normal blowing parameters, maximum local drag reduction and averaged drag reduction and net-power saving of the first Bayesian optimisation. The grey line is the canonical turbulent boundary-layer. The blue line indicates the case with the highest net-power saving. The red line indicates the case with the highest drag reduction over L.

Case BO1	C_B $\times 100$	N_B	α	Max DR	GDR	S_1
0	0	–	–	–	–	–
1	0.5	1	1	52	13.2	3.2
2	0.5	1	0.47	48.5	6.0	1.3
3	0.5	1	0.24	49	2.9	0.6
4	0.37	5	0.9	39.3	9.3	4.3
5	1	10	0.78	75.5	19.8	-9.5
6	0.03	1	1	39.5	0.9	0.9
7	0.42	3	0.95	45	11.0	3.8
8	0.40	6	0.88	41	9.6	3.1
9	0.23	8	0.82	39.5	5.4	3.3
10	0.14	1	0.06	39.5	0.4	0.3
11	0.0	10	0.78	39.5	-0.5	-0.5
12	0.6	10	0.78	54.2	12.3	1.5
13	0.29	1	1	36.3	8.3	5.0
14	0.39	1	1	41	10.4	4.5
15	0.3	1	1	39	8.4	4.8
16	0.29	1	1	39.5	8.1	4.8
17	0.29	1	1	39.5	7.9	4.6
18	0.28	1	1	39.5	7.6	4.5

this blowing device is underestimated as the power required to compress the air is not taken into account. This first BO study is clearly showing that high levels of drag reduction are not necessarily required to generate net-power saving.

Table 2: Wall-normal blowing parameters, maximum local drag reduction and averaged drag reduction and net-power saving of the second Bayesian optimisation. The red row indicate the highest drag reduction, and the blue row is a case for which net-power saving is achieved with intermittent blowing.

Case BO2	C_B $\times 100$	N_B	α	Max DR	GDR	S_2
0	–	–	–	–	–	–
1	0.5	1	1	52	13.2	1.2
2	0.5	1	0.47	48.5	6.0	0.3
3	0.5	1	0.24	49	2.9	0.0
4	0.41	2	0.24	37	2.5	0.2
5	0.51	1	0.25	47.5	3.1	0.2
6	0.7	1	0.23	60.5	4.1	0.5
7	0.42	1	0.22	39	2.2	0.0
8	0.93	5	0.23	51.5	5.6	0.7
9	0.88	4	0.24	55	5.3	0.7
10	0.79	3	0.23	57	4.6	0.5
11	0.80	2	0.23	63.5	4.7	0.6

In BO2, the total power input of the blowing device is taken into account so the evaluation of the net-power saving is more realistic. The first three simulations used the same blowing parameters as in BO1. 11 DNS are carried out for this second BO study. It can be seen that the results are fairly different when compared to the first BO study. Table 2 shows the parameters chosen by the Bayesian optimisation framework as it searches through parameter space to achieve a global skin-friction drag reduction with a net-power saving. After 6 iterations the Bayesian optimisation framework predicts that a short intense uniform blowing strategy will achieve a local maximum skin-friction drag reduction of 60.5% and a global skin-friction drag reduction of 4.1% with a net-power saving of 0.5% (Case 6 in blue). Interestingly, it is also possible to generate a net-power saving of 0.7% (Case 8 in red) with an intermittent blowing and low intensity blowing. The highest net-power saving is achieved in Case 1 with more than 1% of net-power saving.

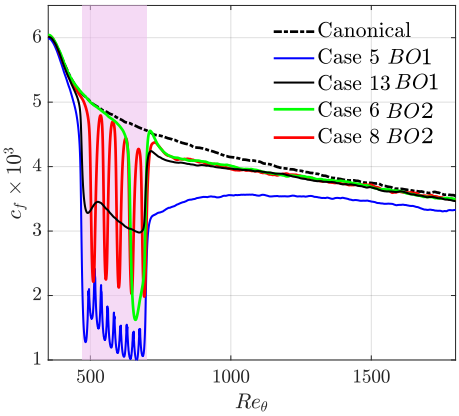

Figure 3: Streamwise evolution of the friction coefficient.

The local skin-friction coefficient versus Re_θ is plotted in figure 3. It can be seen that most of the drag reduction is achieve over the control area (in pink). It can be seen that the drag reduction persists for several hundred boundary-layer thicknesses downstream of control with a slow spatial recovery back to the canonical case. These results are consistent with previously published numerical data in a similar set-up (Stroh *et al.* (2016)). This figure highlights the fact that the BO framework has the potential to find different sets of parameters to achieve net-power saving and that the long lasting drag reduction effect downstream of the control area is responsible for the net-power saving.

FIK identity

Fukagata *et al.* (2002) derived an expression of the skin-friction coefficient for incompressible turbulent flows. Their expression is known as the Fukagata-Iwamoto-Kasagi (FIK) identity. For spatially developing boundary layers which are homogeneous in the spanwise direction, the FIK identity can be expressed as

$$c_f^{FIK}(x) = \underbrace{\frac{4(1-\delta^*)}{Re_\delta}}_{c_f^\delta} + \underbrace{4\int_0^1 (1-y)(-\overline{u'v'})dy}_{c_f^T} + \underbrace{4\int_0^1 (1-y)(-\bar{u}\bar{v})dy}_{c_f^C} \underbrace{-2\int_0^1 (1-y)^2\left(\frac{\partial \bar{u}\bar{u}}{\partial x} + \frac{\partial \overline{u'u'}}{\partial x} - \frac{1}{Re_\delta}\frac{\partial^2 \bar{u}}{\partial x^2} + \frac{\partial \bar{p}}{\partial x}\right)dy}_{c_f^D}, \quad (5)$$

where $\bar{\cdot}$ denotes the Reynolds-averaged quantities, δ^* is the displacement thickness and $Re_\delta = \frac{U_\infty \delta}{\nu}$. All the dimensions, δ^*, x and y are normalized by the local boundary layer thickness δ. The FIK identity decomposes the friction coefficient into four terms: a contribution from boundary layer thickness c_f^δ, a Reynolds shear stress contribution c_f^T, a mean wall-normal convection contribution c_f^C and a spatial development contribution c_f^D.

The streamwise average of the FIK identity terms in the control region ($Re_\theta = 470:700$) and downstream of it ($Re_\theta = 700:1400$) for the canonical case, Case 13 and Case 5 from BO1 are reported in figure 4. First, we can see that the friction coefficients calculated by the streamwise shear stress, c_f (in red), match the ones calculated by the FIK identity, c_f^{FIK} (in back dashed lines). To obtain drag reduction in the control region, the increase for c_f^D and c_f^T needs to be counteracted by a strong reduction for c_f^C. The significant growth of the magnitude of c_f^C can be associated with the increase of the vertical velocity in the blowing section. An intriguing observation is related to the increase of c_f^C and the reduction of c_f^D downstream of the blowing region which may revert their sign, for example Case 5. It is possible to conclude that over the blowing region the reduction of the convection contribution c_f^C is responsible for the total drag reduction, while the spatial development contribution c_f^D is responsible for the low drag observed downstream of the blowing region.

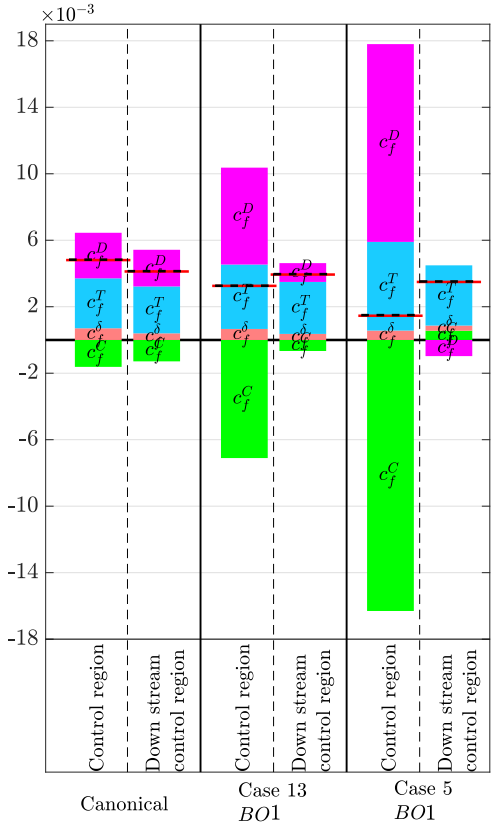

Figure 4: Streamwise average of the FIK identity terms in the control region and downstream of it for the canonical case, Case 5 and Case 13 from BO1. Black dashed line is the sum of all the FIK identity terms.

LES study

In this section, we investigate the possibility of using ILES instead of DNS for future BO studies. As observed in figure 5, there is a very good agreement between the ILES data and the DNS data with and without blowing (Cases 5 and 13 from BO1). The friction coefficient obtained, which is used for our BO studies, is correctly predicted by our ILES, within 5% of the DNS data. We can therefore conclude that ILES can be used for future BO studies in order to drastically reduced the cost of the optimisation (in our case by a factor 16).

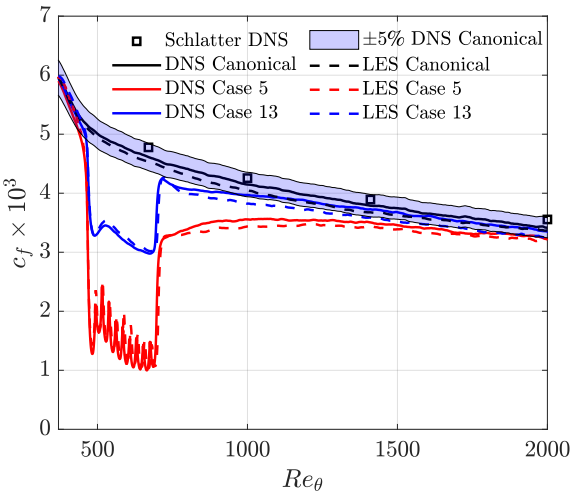

Figure 5: Comparison between DNS and ILES data for the streamwise evolution of the skin-friction coefficient for the canonical case and cases 5 and 13 from the first BO study. For completeness, the canonical TBL data from Schlatter & Örlü (2010) are plotted with the black square symbols.

Future work

In our quest to improve net-power saving, it would be a good idea to increase the number of parameters for the BO algorithm. In order to find the potentially important parameters for future BO studies, we decided to investigate with few ILES the influence of time dependence for C_B. This potential time modulation can be controlled by two parameters: $f_B = 1/T_m$ which corresponds to the time frequency of the modulation ($T_m = 0.5, 1$ and $4\delta_0/U_\infty$), and DC which correspond to the duty cycle for the modulation. Steady blowing is applied when DC=100%. It can be hypothesised that net-power saving could potentially be increased by reducing the time during which the blowing is on while hopefully sustaining a high enough drag reduction over and downstream of the control area. 7 ILES are therefore performed for this study. The results are presented in Table 3. The first important results is that the data for Case 1 and Case 4 of the ILES study are similar to the one obtained in the first BO study (Case 13 and Case 5, respectively) based on DNS data. Different blowing frequencies are tested and it is found that there is a correlation between the intensity of the blowing C_B and the duty cycle of the modulation DC: similar drag reduction levels are achieved for Cases 2/3 and Cases 5-7. The drag reduction level obtained by a 50% time modulation is the same as the one obtained by reducing the intensity of the blowing by half. It can also be seen that in a context of streamwise intermittent blowing, the time modulation has virtually no effect on the drag reduction. It

Table 3: Wall-normal blowing parameters, maximum local drag reduction and averaged drag reduction over L and net-power saving of the ILES study using the two different blowing systems.

Case TEST3	C_B $\times 100$	N_B	α	f_B	DC(%)	Max DR	GDR	S_1	S_2
1	0.29	1	1	1	100	34.2	-8.1	4.5	-0.1
2	0.29	1	1	2	50	19.1	-4.0	2.2	-0.1
3	0.145	1	1	1	100	18.7	-4.0	3.1	-0.5
4	1	10	0.78	1	100	77.2	-20.6	-10.7	0.4
5	1	10	0.78	0.25	50	48	-10.1	-6.4	0.01
6	1	10	0.78	2	50	48.4	-10.2	-6.3	0.1
7	0.5	10	0.78	1	100	47.4	-10.1	1.86	0.2

seems to suggest that adding a time modulation parameters to future BO studies might not be relevant to achieve higher net-power savings.

Conclusion

In this work, DNS of a specially developing turbulent boundary layer with continuous/discontinuous wall blowing were performed to provide data for a Bayesian Optimisation algorithm, and used to find the optimal parameters to generate net-power saving by reducing the friction coefficient of the boundary layer. Two BO studies were carried out, one with the experimental data of Kornilov & Boiko (2012) and one with a new low cost wall blowing solution using mini speakers. The results are very promising and future studies will address the relatively low net-power saving by increasing the streamwise extent of the control region, by increasing the Reynolds numbers and by increasing the number of parameters for the BO algorithm. Instead of using costly DNS, these future studies will be based on ILES, which will drastically reduce the cost of the optimisation.

Acknowledgements

The authors would like to thank EPSRC for the computational time made available on the UK supercomputing facility ARCHER via the UK Turbulence Consortium (EP/L000261/1). The authors also acknowledge PRACE for awarding them access to Hazel Hen at HLRS, Germany (project 2018184381). Omar Mahfoze would like to thank Imperial College for funding his PhD with an Imperial College President Scholarship.

REFERENCES

Brochu, Eric, Cora, Vlad M & De Freitas, Nando 2010 A tutorial on bayesian optimization of expensive cost functions, with application to active user modeling and hierarchical reinforcement learning. *arXiv preprint arXiv:1012.2599* .

Dairay, T., Lamballais, E., Laizet, S. & Vassilicos, J.C. 2017 Numerical dissipation vs. subgrid-scale modelling for Large Eddy Simulation. *Journal of Computational Physics* **337**, 252–274.

Diaz-Daniel, Carlos, Laizet, Sylvain & Vassilicos, J Christos 2017 Wall shear stress fluctuations: Mixed scaling and their effects on velocity fluctuations in a turbulent boundary layer. *Physics of Fluids* **29** (5), 055102.

Fukagata, Koji, Iwamoto, Kaoru & Kasagi, Nobuhide 2002 Contribution of reynolds stress distribution to the skin friction in wall-bounded flows. *Physics of Fluids* **14** (11), L73–L76.

Gelbart, Michael A, Snoek, Jasper & Adams, Ryan P 2014 Bayesian optimization with unknown constraints. *arXiv preprint arXiv:1403.5607* .

Kametani, Yukinori & Fukagata, Koji 2011 Direct Numerical Simulation of spatially developing turbulent boundary layers with uniform blowing or suction. *Journal of Fluid Mechanics* **681**, 154–172.

Kametani, Yukinori, Fukagata, Koji, Örlü, Ramis & Schlatter, Philipp 2016 Drag reduction in spatially developing turbulent boundary layers by spatially intermittent blowing at constant mass-flux. *Journal of Turbulence* **17** (10), 913–929.

Kornilov, Vladimir I & Boiko, Andrey V 2012 Efficiency of air microblowing through microperforated wall for flat plate drag reduction. *AIAA journal* **50** (3), 724–732.

Laizet, Sylvain & Lamballais, Eric 2009 High-order compact schemes for incompressible flows: A simple and efficient method with quasi-spectral accuracy. *Journal of Computational Physics* **228** (16), 5989–6015.

Laizet, Sylvain & Li, Ning 2011 Incompact3d: a powerful tool to tackle turbulence problems with up to $0(10^5)$ computational cores. *Int. Journal for Numerical Methods in Fluids* **67** (11), 1735–1757.

Schlatter, Philipp & Örlü, Ramis 2010 Assessment of direct numerical simulation data of turbulent boundary layers. *Journal of Fluid Mechanics* **659**, 116–126.

Snoek, Jasper, Larochelle, Hugo & Adams, Ryan P 2012 Practical bayesian optimization of machine learning algorithms. In *Advances in neural information processing systems*, pp. 2951–2959.

Stroh, A, Hasegawa, Y, Schlatter, Philipp & Frohnapfel, B 2016 Global effect of local skin friction drag reduction in spatially developing turbulent boundary layer. *Journal of Fluid Mechanics* **805**, 303–321.

Virk, Preetinder S 1975 Drag reduction fundamentals. *AIChE Journal* **21** (4), 625–656.